

DESIGN OF CRACK ARRESTORS FOR ULTRA HIGH GRADE GAS TRANSMISSION PIPELINES SIMULATION OF CRACK INITIATION, PROPAGATION AND ARREST

F. Van den Abeele¹, M. Di Biagio² and L. Amlung³

¹ OCAS N.V., J.F. Kennedylaan 3, 9060 Zelzate, Belgium

² Centro Sviluppo Materiali, Rome, Italy

³ RWTH Aachen University, Aachen, Germany

Abstract

One of the major challenges in the design of ultra high grade (X100) gas pipelines is the identification of a reliable crack propagation strategy. Recent research results have shown that the newly developed high strength and large diameter gas pipelines, when operated at severe conditions, may not be able to arrest a running ductile crack through pipe material properties. Hence, the use of crack arrestors is required in the design of safe and reliable pipeline systems.

A conventional crack arrestor can be a high toughness pipe insert, or a local joint with higher wall thickness. According to experimental results of full-scale burst tests, composite crack arrestors are one of the most promising technologies. Such crack arrestors are made of fibre reinforced plastics which provide the pipe with an additional hoop constraint. In this paper, numerical tools to simulate crack initiation, propagation and arrest in composite crack arrestors are introduced.

First, the in-use behaviour of composite crack arrestors is evaluated by means of large scale tensile tests and four point bending experiments. The ability of different stress based orthotropic failure measures to predict the onset of material degradation is compared. Then, computational fracture mechanics is applied to simulate ductile crack propagation in high pressure gas pipelines, and the corresponding crack growth in the composite arrestor. The combination of numerical simulation and experimental research allows deriving design guidelines for composite crack arrestors.

Keywords crack arrestors, toughness modelling, pipeline materials, fibre reinforced plastics, integrity

1 INTRODUCTION: COMPOSITE CRACK ARRESTORS

The occurrence of a longitudinal crack propagating along a gas pipeline is a catastrophic event, which involves both economic losses and environmental damage. Hence, the fracture propagation control is an essential strategy to ensure pipeline integrity. Fracture control is a tough task, since it requires knowledge of the interaction between the dynamic forces driving crack growth, and the resistance forces opposing fracture propagation.

While brittle fracture control is typically achieved by ensuring that the pipeline is operated well above the Ductile to Brittle Transition Temperature, the ductile fracture propagation can be avoided (or at least limited) by increasing the minimum specified toughness of the pipeline steel. However, for ultra high pipeline grades (\geq X100), the identification of a reliable crack propagation strategy is not longer straightforward. Indeed, despite excellent toughness values at lab scale (Charpy upper shelf energy and Battelle shear fracture area), one can no longer rely on pipe body arrest [1-3]. As a result, additional mechanical devices such as crack arrestors have to be mounted on the pipeline in order to stop a running ductile crack.

According to experimental results of full-scale burst tests, it is argued [4] that the most promising materials are

- *Steel sleeve arrestors*, in particular *tight* sleeves, which are placed around the main linepipe with a close fitting connection
- *Composite arrestors*, made of fibre reinforced plastics which provide the pipe with an additional hoop constraint.

In an accompanying paper [5], the requirements for material selection, testing and modelling were reviewed for the design of crack arrestors for ultra high grade gas transmission pipelines. For composite arrestors, uni-directional glass fibre reinforced epoxy was identified as the best balance between mechanical properties and cost considerations. Traditional mechanical characterization was performed to determine the orthotropic properties: both tensile tests, compression tests and three rail shear tests were conducted in fibre direction and in transverse direction. The in-plane elastic properties were determined by a dynamic identification technique using resonant frequencies as well. The elastic properties, obtained with this non destructive testing method, are homogenised over the plate surface, and hence suitable as averaged input values in finite element models for composite structures. Several micromechanical mixture rules to calculate the elastic constants of the unidirectional laminate were proposed in [6]. The Hashin model, which has been derived for unidirectional reinforced composites, shows the best agreement with the experimental data.

In this paper, numerical techniques to simulate subsequent crack initiation, propagation and arrest are introduced. First, the in-use behaviour of composite crack arrestors is evaluated by means of large scale tensile tests and four point bending experiments. The ability of different stress based orthotropic failure measures to predict the onset of material degradation is compared. Then, computational fracture mechanics is applied to simulate ductile crack propagation in high pressure gas pipelines, and the corresponding crack growth in the composite arrestor. For the finite element simulations of the composite crack arrestor, the initial material properties obtained in [5] and listed in Table 1 are used.

Table 1: Stiffness and strength values used in the finite element simulations

E_1 44 200 MPa	$E_2 = E_3$ 11 400 MPa	$\nu_{12} = \nu_{13}$ 0.356	ν_{23} 0.343	$G_{12} = G_{13}$ 4 420 MPa	G_{23} 5 027 MPa
X_T 700 MPa	Y_T 7.2 MPa	X_C 588 MPa	Y_C 42 MPa	R 30.1 MPa	S 30.1 MPa

2 IN-SERVICE BEHAVIOUR OF COMPOSITE CRACK ARRESTORS

When a pipeline is being installed, the crack arrestor can be subjected to tensile loads and bending stresses. In addition, during the operational life of the pipeline system, the composite crack arrestor is exposed to environmental loads, low temperatures, external damage, fatigue, ...

In order to evaluate the in-service behaviour of composite arrestors, an extensive testing program was undertaken, including three and four point bending experiments and tensile tests at different temperatures. In addition, low cycle fatigue and ageing were studied as well. For these experiments, the behaviour of a unidirectional reinforced crack arrestor was compared with an arrestor with a winding pattern including inclined fibres, contributing to the axial reinforcement. The winding patterns are compared on Figure 1.

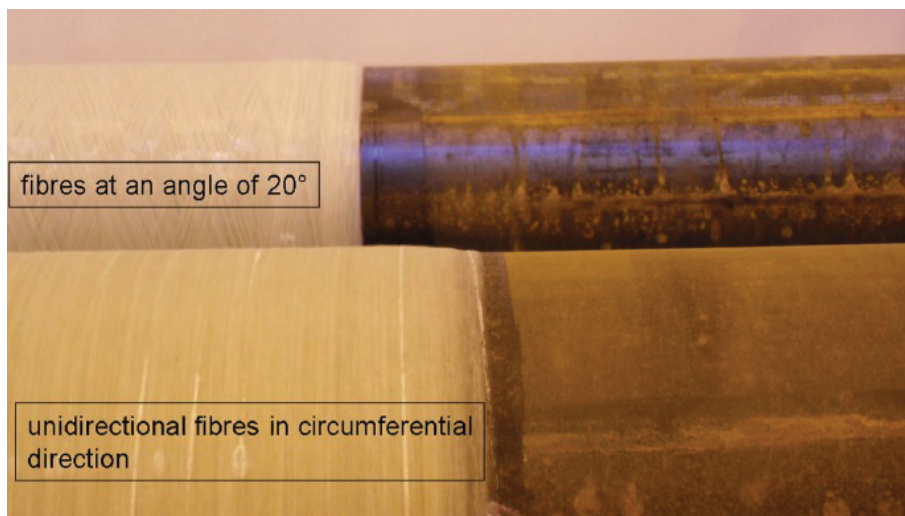


Figure 1: Different winding patterns for the composite crack arrestors

2.1 Tensile tests

Tensile tests were performed on a medium scale S235 steel pipe (with length $L = 4$ m, outer diameter $D = 220$ mm and wall thickness $t = 3.2$ mm). The length of the composite crack arrestor was $L_a = 660$ mm, and the thickness of the windings was $t_a = 4.8$ mm. The tensile test setup is shown on Figure 2. For the quasi-static tensile tests at lower temperatures (-30°C), a local cooling box is installed around the crack arrestor.

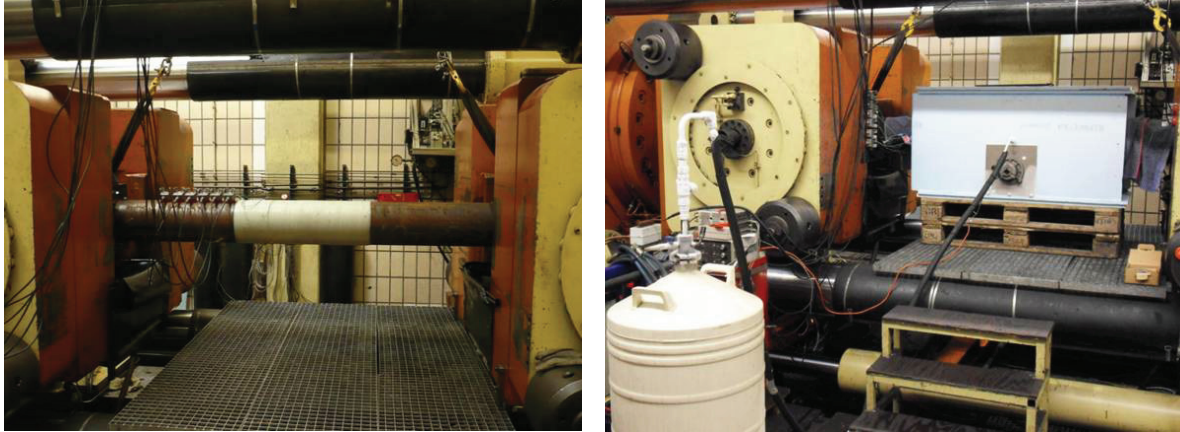


Figure 2: Tensile test setup for room temperature (left) and lower temperatures (right)

In order to enable a proper introduction of the load to the pipe, the ends were furnished with flanges, which were fastened to a clamping support, like shown on Figure 3. During the experiment, the applied force and the piston displacement were measured. In addition, several strain gauges (shown on Figure 3) were attached to the steel pipe and the composite crack arrestor to monitor local deformations.



Figure 3: Clamping support (left) and strain gauge arrangement (right)

On Figure 4, typical load-displacement curves for the tensile tests are shown. The blue curve shows the response of a unidirectional reinforced crack arrestor at room temperature, while the red curve corresponds to the same crack arrestor tested at lower (-30°C) temperature. The hysteresis in this red curve indicates unloading during the experiment, in order to allow visual examination of the composite surface.

For the unidirectional crack arrestor, failure is initiated in the first third of the test period. The strain measurements on the crack arrestor surface indicate failure at a critical failure strain $\varepsilon_c \approx 0.08\%$, which is in very close agreement with the coupon testing reported in [7].

The strain gauge measurements reveal that the crack arrestor material fails when the tensile strength in transverse direction is reached. In some experiments, an increase in hoop strain could be observed, which might indicate the end of contraction due to debonding.

The blue curve on Figure 4 corresponds to the tensile test at room temperature for a crack arrestor with an inclined winding pattern. Here, unidirectional reinforcement is combined with layers of $\pm 20^\circ$ orientation.

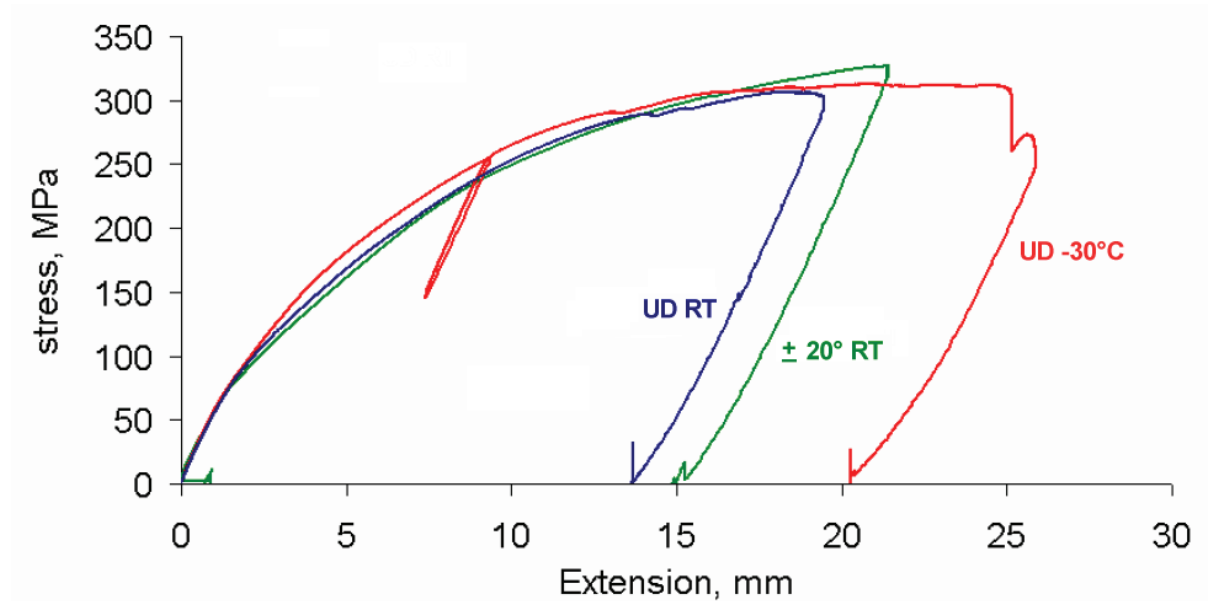


Figure 4: Load-deflection curves for static tensile tests on crack arrestors

Thanks to this axial reinforcement, the inclined winding pattern has a higher resistance to pure tensile loading. The higher strain capacity of the inclined rovings is demonstrated in Figure 5 as well, where the signals of the axial strain gauges are compared with the unidirectional crack arrestor. For the unidirectional reinforcement, failure of the epoxy resin initiated at stress levels close to the yielding point of the parent pipe.

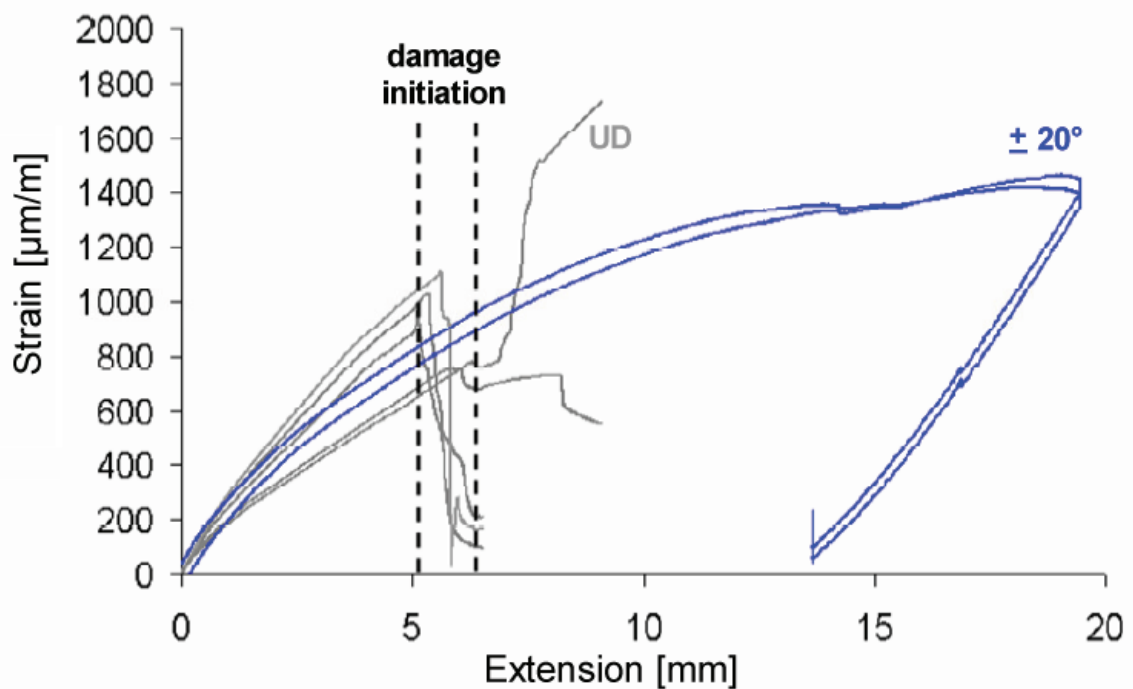


Figure 5: Comparison of axial strains on unidirectional crack arrestor and inclined winding pattern

Although the strain gauges clearly indicated composite material failure, no macroscopic damage could be observed after the experiments. Dye penetrant testing revealed the exact location of the cracks due to tensile loading. On Figure 6, the results of such a dye penetrant inspection are shown. The tested specimen is shown before (left) and after (right) a developer has been applied to reveal the penetrant, and hence the location of the surface-breaking cracks.

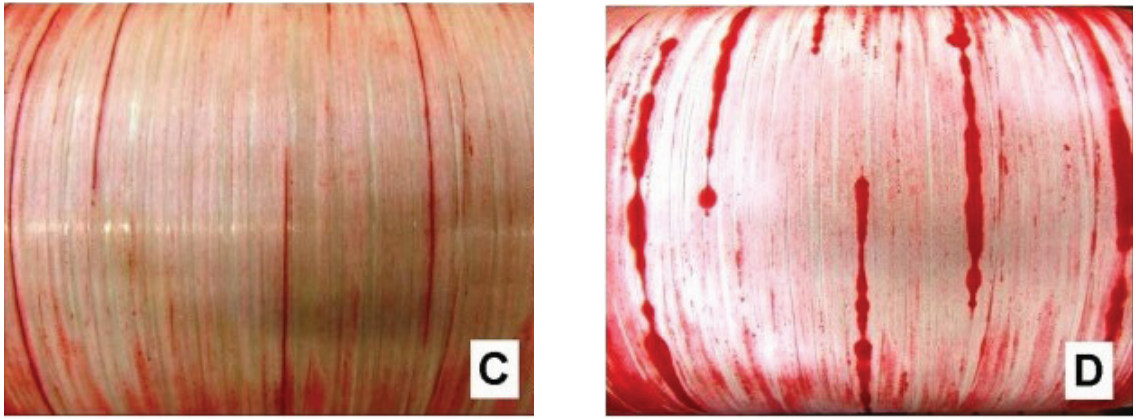


Figure 6: Dye penetrant testing without (left) and with (right) developer to reveal material damage

2.2 Bending experiments

Four point bending tests were performed to assess the response of the composite crack arrestors to combined loading. The experimental setup is shown on Figure 7: the sample is subjected to four point bending, and the load is applied adjacent to the crack arrestor. The applied load and the piston displacement are measured, and strain gauges are applied to monitor local deformations.



Figure 7: Four point bending setup (left) and strain gauge arrangement (right)

Typical results for bending tests at ambient and lower (-30°C) temperatures are shown on Figure 8, where the applied load is shown as a function of the measured piston displacement.

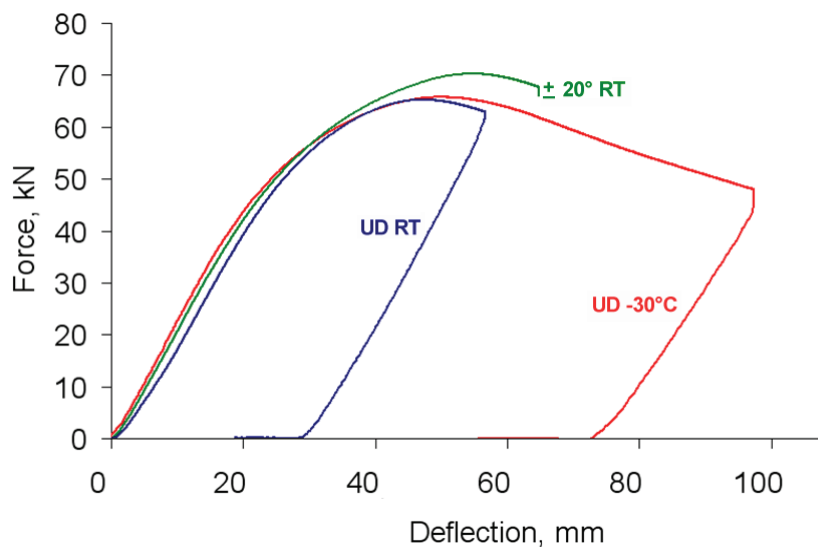


Figure 8: Load-deflection curves for quasi-static four point bending tests

Again, the additional inclined rovings provide additional strength as compared to the unidirectional reinforced crack arrestor. For the UD arrestor, strain gauge measurements revealed that failure occurred at a critical strain $\varepsilon_c \approx 0.1\%$. The measured signals from the transverse strain gauges are shown on Figure 9. The onset of a circumferential crack in the composite material was captured with a camera, and is clearly shown in this picture as well.

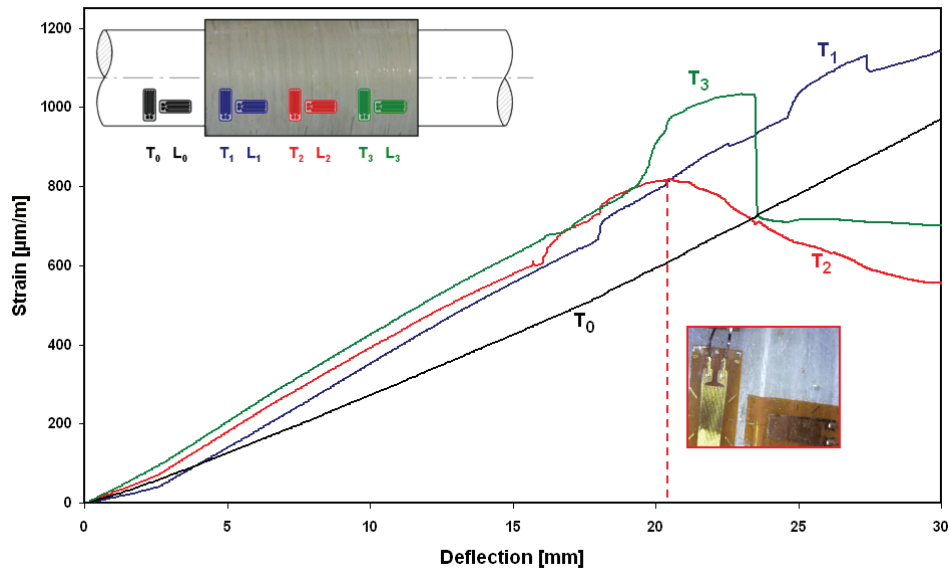


Figure 9: Transverse strain gauge measurements and circumferential crack initiation

2.3 Cyclic bending tests

In order to investigate the influence of low cycle fatigue (induced by cyclic stresses e.g. caused by an earthquake), cyclic four point bending tests were performed. The load input is based on the recommended test procedure [8] of the ECCS. In this case, an increasing alternating load, starting in the elastic range and moving into the plastic range, is applied. This load-time history is shown on Figure 10, together with the corresponding strain gauge measurements on the crack arrestor surface.

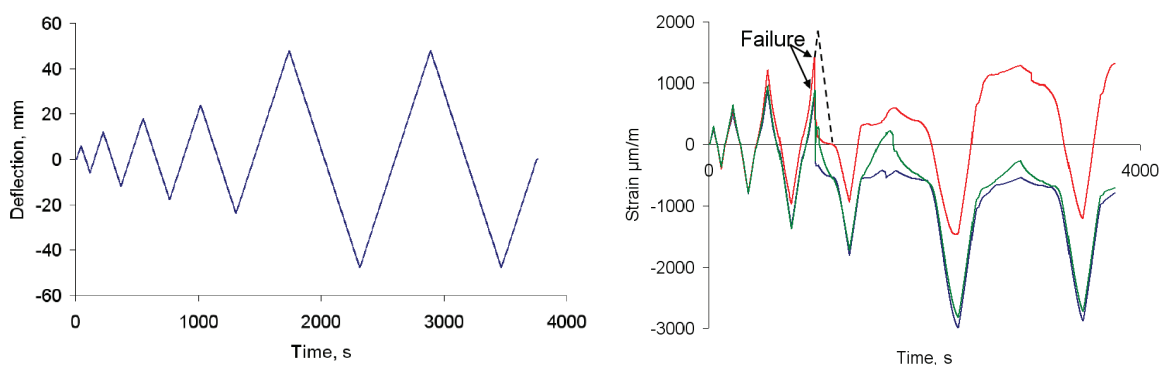


Figure 10: Load time history (left) and strain gauge signals (right) for cyclic four point bending tests

The ends of the test specimens were fixed using bolts, and the load was applied through half-shell shaped supports. The resulting load-deflection curve for a cyclic four point bending test is shown on Figure 11, indicating that the maximum bending force is slightly higher than in the static bending tests. For the unidirectional reinforced crack arrestors, failure of the epoxy resin –similar to the failure mode for the monotonic experiments- could be observed. The onset of composite material failure is clearly captured by the strain gauges, like shown on Figure 10. Crack closure during the compressive stress cycles contributes to an increased failure strain. During the cyclic bending tests, no separation between the steel pipe and the composite crack arrestor could be observed, indicating that monotonic load assumptions are justified to design composite crack arrestors to withstand ultra low cycle fatigue loading.

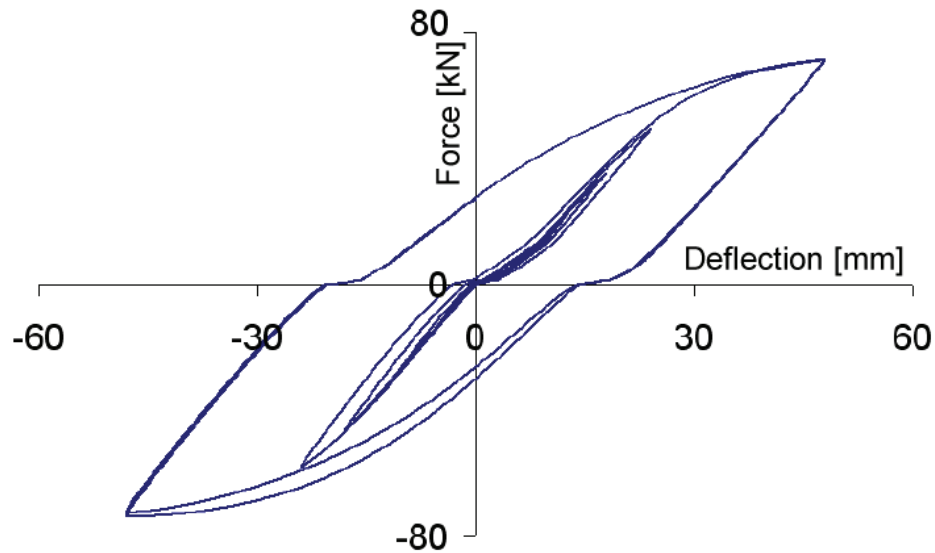


Figure 11: Load-deflection curve for a cyclic four point bending test

3 ORTHOTROPIC FAILURE MEASURES TO PREDICT THE ONSET OF FAILURE

Orthotropic (plane stress) failure measures are indications of composite material degradation, where a sound material has an index $I_F = 0.0$ and a failed material has an index $I_F = 1.0$. The orthotropic linear elastic behaviour can be extended with a failure envelope, according to different criteria. In [6], the ability of different orthotropic failure measures was presented, and their ability to describe failure for composite crack arrestors was evaluated. The criterion of Hashin [9] and Rotem [10] was identified as the best failure measure for unidirectional reinforced composites.

To predict damage initiation, Hashin and Rotem propose four different criteria to distinguish between matrix and fibre failure in tension and compression. For fibre rupture in tension ($\sigma_{11} > 0$), they suggest

$$F^T = \left(\frac{\sigma_{11}}{X_T} \right)^2 + \frac{\tau_{12}^2 + \tau_{13}^2}{S^2} < 1 \quad (\text{Eq. 01})$$

while

$$F^C = \left(\frac{\sigma_{11}}{X_C} \right)^2 + \frac{\tau_{12}^2 + \tau_{13}^2}{S^2} < 1 \quad (\text{Eq. 02})$$

is proposed for fibre buckling/kinking in compression ($\sigma_{11} < 0$). The initiation criterion for matrix cracking under transverse tension and shearing ($\sigma_{22} + \sigma_{33} > 0$) reads

$$M^T = \left(\frac{\sigma_{11} + \sigma_{33}}{Y_T} \right)^2 + \frac{\tau_{23}^2 - \sigma_{22} \sigma_{33}}{T^2} < 1 \quad (\text{Eq. 03})$$

and compressive matrix damage ($\sigma_{22} + \sigma_{33} < 0$) is described by

$$M^C = \frac{\sigma_{22} + \sigma_{33}}{Y_C} \left[\left(\frac{Y_C}{2T} \right)^2 - 1 \right] + \frac{(\sigma_{22} + \sigma_{33})^2}{4T^2} + \frac{\sigma_{23}^2 - \sigma_{22} \sigma_{33}}{T^2} + \frac{\tau_{12}^2 + \tau_{13}^2}{S^2} < 1 \quad (\text{Eq. 04})$$

These failure measures are used to define the internal variables that characterize fibre damage

$$d_f = \begin{cases} F^T & ; \hat{\sigma}_{11} \geq 0 \\ F^C & ; \hat{\sigma}_{11} < 0 \end{cases} \quad (\text{Eq. 05})$$

matrix damage

$$d_f = \begin{cases} F^T & ; \hat{\sigma}_{11} \geq 0 \\ F^C & ; \hat{\sigma}_{11} < 0 \end{cases} \quad (\text{Eq. 06})$$

and shear damage

$$d_s = 1 - (1 - F^T)(1 - F^C)(1 - M^T)(1 - M^C) \quad (\text{Eq. 07})$$

respectively, where the effective stress tensor $\hat{\sigma} = D \sigma$ is computed from the damage operator

$$D = \begin{bmatrix} \frac{1}{1-d_f} & 0 & 0 \\ 0 & \frac{1}{1-d_m} & 0 \\ 0 & 0 & \frac{1}{1-d_s} \end{bmatrix} \quad (\text{Eq. 08})$$

The damage initiation criteria (Eq. 01) - (Eq. 04) according to Hashin are implemented in a finite element model of the four point bending tests reported in the previous section. The pipe is modelled as a deformable solid, with three elements through the thickness to accurately capture the bending stresses. The unidirectional reinforced epoxy is modelled as an orthotropic composite material, with the elastic properties of Table 1. The total problem size was 48 678 elements and 212 052 degrees of freedom. In Figure 12, the four point bending simulation is compared with the experimental curve, indicating that the tensile matrix cracking criterion $M^T = 1$ is capable of predicting the onset of damage in the composite crack arrester.

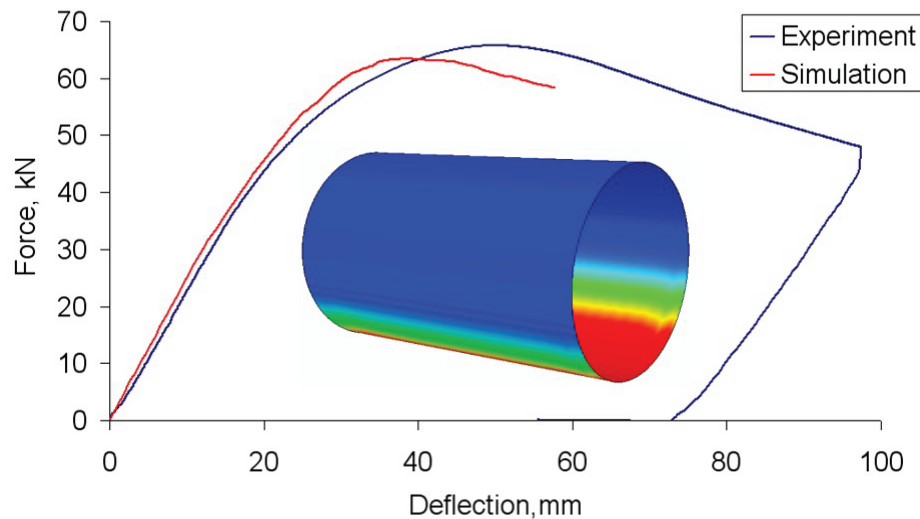


Figure 12: Four point bending simulation with the Hashin tensile matrix cracking criterion

4 SIMULATION OF DUCTILE CRACK PROPAGATION

For the simulation of ductile crack propagation in high pressure gas pipelines, the PICPRO (Pipe Crack Propagation) code, developed by CSM and the University of Rome [11-12] was used. The model uses an explicit integration algorithm based on a central difference scheme. As a result, it is able to take both steady-state and transient fracture propagation conditions into account during the analysis, including abrupt changes of constraint characteristics such as those which occur in the vicinity of crack arrestors.

The code also accounts for local strain rate effects [12], soil constraint effects [13] and decompression of the gas flowing through the fracture breach according to the actual gas composition, pressure and temperature. Material ductility is described by a Fracture Process Zone, which is explained in [14-15].

A special feature of PICPRO is the integration of a numerical model which accounts for the presence of a crack arrestor mounted on the pipeline, and the resulting effect on a running shear fracture. An interaction algorithm is used to simulate the constraint effect exerted by the crack arrestor, and a modified gas decompression curve is used to account for the dynamic effect of the crack arrestor. The Hashin progressive damage model is used to predict crack propagation in the composite material.

The finite element code simulates dynamic ductile fracture propagation in a high pressure gas pipeline by estimating the arrest/propagation condition on the basis of an equilibrium between the fracture driving force (calculated by the PICPRO code itself) and the resistance force of the material under consideration (i.e. the toughness of the linepipe steel and the additional constraint of the composite crack arrestor).

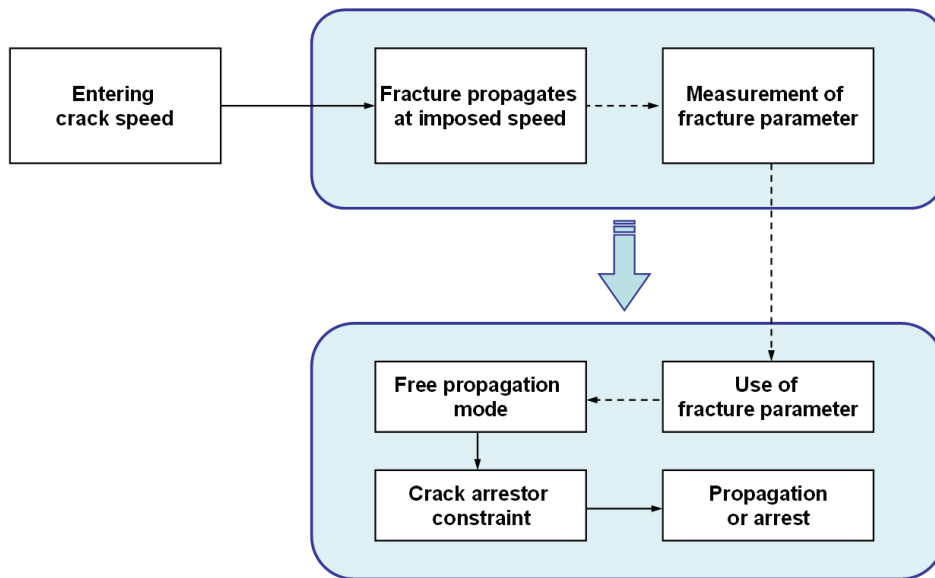


Figure 13: Flowchart for finite element simulation of crack propagation

When simulating crack arrestors, evaluating the effect of abrupt changes in constraint conditions (e.g. thickness variations of the composite crack arrestor for different winding patterns) is important to accurately predict the fracture propagation and/or arrest. The flowchart on Figure 13 shows the finite element procedure followed by the PICPRO program. An initial crack speed is imposed on the steel pipe, based on experimental data [15]. Just before the crack enters the crack arrestor, the specific energy consumed for fracture advance is evaluated and stored as a measure of the inherent pipe fracture resistance related to the initial imposed crack speed. From this point on, crack advance is governed by the free propagation algorithm [14]. When the fracture enters the crack arrestor, the variation in the external constraint will cause deceleration and, if the crack arrestor is properly designed, arrest. In the next section, the versatility of this numerical tool to design composite crack arrestors is demonstrated.

5 DESIGN GUIDELINES FOR COMPOSITE CRACK ARRESTORS

The combination of numerical simulation and experimental research allows deriving design guidelines for composite crack arrestors. In this section, the Hashin damage model for the composite material is combined with the PICPRO code to simulate ductile crack propagation, which enables to design 'fit for purpose' composite crack arrestors. First, the numerical tools are applied to calculate the optimum dimensions (thickness and length) of a composite crack arrestor for a small-scale pipe. Then, the method is extended to predict crack arrest in a full-scale burst test of a 36" natural gas pipeline.

5.1 Design of crack arrestor thickness

The finite element model is first applied to simulate a running shear fracture in a small-scale X100 pipe (diameter 75 mm, wall thickness 1.5 mm) for different crack arrestor geometries. The diameter/wall thickness range is 50, which lays within the typical range of pipes for gas transportation. The crack arrestor length was 150 mm, and a burial depth of 35 mm is considered to provide the pipe with a more realistic backfill constraint action. The arrestor is located at a distance of 0.8 meters from the crack initiation site. The simulations have been performed using air as pressurizing medium and by imposing the burst pressure at a value corresponding to 80% of X100 specified minimum yield stress.

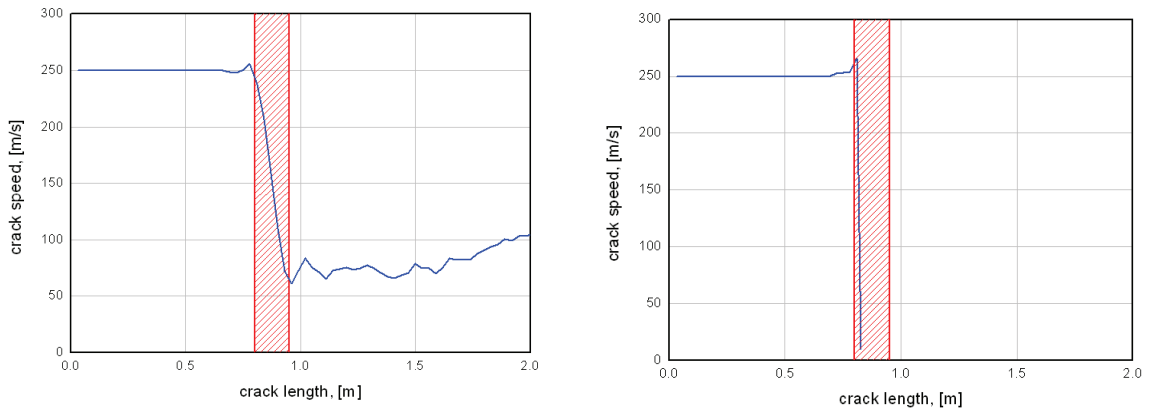


Figure 14: Predicted crack speed diagrams for $t_a = 1.5$ mm (left) and $t_a = 3.0$ mm (right)

For a composite reinforcement with a thickness of 1.5 mm (i.e. equal to the pipe wall thickness), no crack arrest is predicted. As shown in the crack speed diagram of Figure 14, the crack is initially imposed to propagate at a speed of 250 m/s, for an internal pressure of 220 bar. When entering the composite crack arrestor, the fracture speed is predicted to slow down to ca. 70 m/s, but propagates further with an increasing speed. The composite reinforcement is predicted to be totally destroyed and proves ineffective in arresting the fracture. When increasing the thickness of the crack arrestor to 3.0 mm, the simulated fracture is effectively slowed down and crack arrest is predicted.

5.2 Design of crack arrestor length

Similar simulations can be performed to calculate the optimum crack arrestor length. For an internal pressure of 200 bar and a composite thickness of 2.0 mm, the performance of a long crack arrestor ($L = 150$ mm) is compared to the behaviour of a short crack arrestor ($L = 37.5$ mm) on Figure 15.

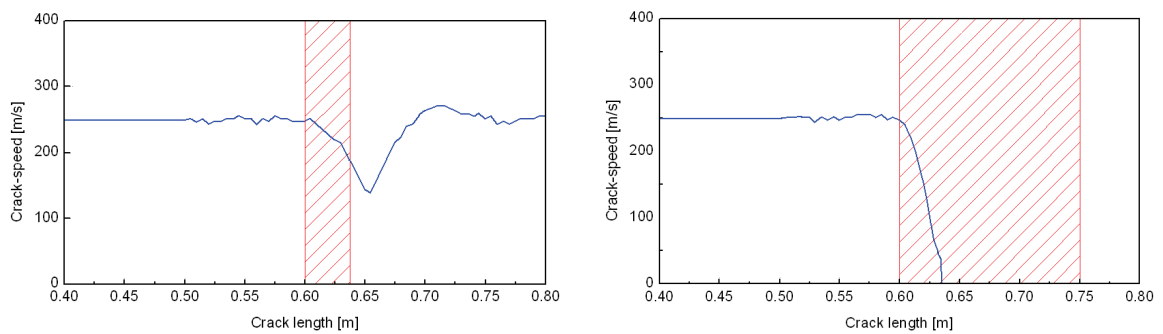


Figure 15: Predicted crack speed diagrams for $L_a = 37.5$ mm (left) and $L_a = 150$ mm (right)

Although the crack speed is considerably decreased in the short arrestor, by virtue of the constraint action exerted by the composite windings, the crack arrestor length is not sufficient to stop the running fracture. When the length is increased to 150 mm, crack arrest is achieved within 35 mm. The composite material damage predicted by the finite element analysis is compared in Figure 16.

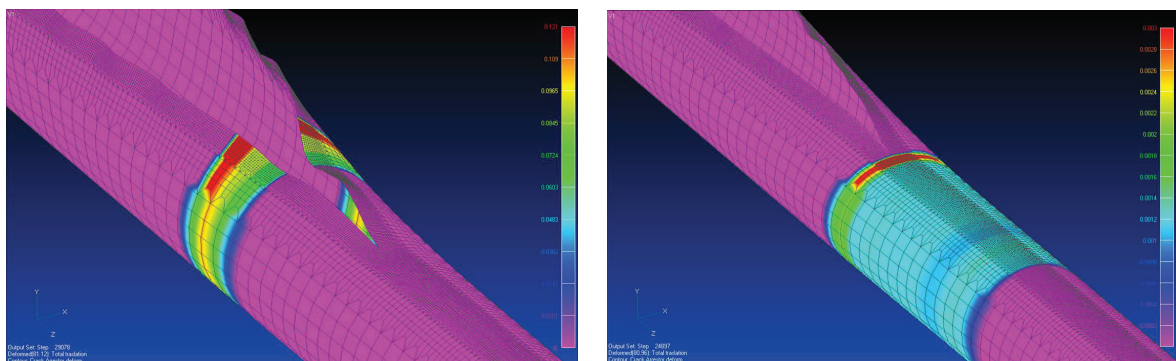


Figure 16: Predicted composite material damage for $L_a = 37.5$ mm (left) and $L_a = 150$ mm (right)

5.3 Crack arrestor design for full-scale burst test

As a final validation, one of the full-scale burst tests performed during the Demopipe [16] project is simulated. The parameters for the experiment are summarized in Table 2. The composite crack arrestor, made out of unidirectional glass fibre reinforced epoxy, is shown on Figure 17 before and after the experiment.

Table 2: Data for the Demopipe full-scale burst test

PIPE		
Outer diameter	[“]	36
Wall thickness	[mm]	20.0
Burial depth	[mm]	1.5
MATERIAL		
Grade	API 5L	X100
Elongation	[%]	16.5
Yield Stress	[MPa]	760
Tensile strength	[MPa]	813
GAS		
Pressurizing medium		natural gas
Burst pressure	[bar]	226
Temperature	[°C]	14
CRACK ARRESTOR		
Length	[mm]	1 600
Thickness	[mm]	40.0
Ultimate strength	[MPa]	826.8
Ultimate strain	[-]	0.018
Crack speed	[m/s]	135
EXPERIMENTAL RESULT		
arrest within 0.5 m		

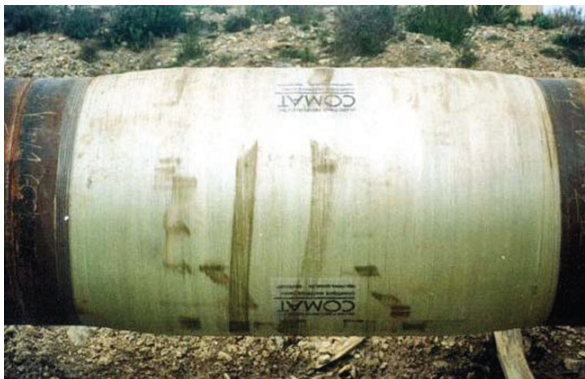


Figure 17: Demopipe composite crack arrestor before and after full-scale burst test [16]

With the settings listed in Table 2, the full-scale burst test was simulated using the PICPRO code and the Hashin damage model. The results are shown in Figure 18: the Critical Crack Tip Opening Angle ($CTOA_C$) is predicted as 5.4° . The imposed crack speed of 135 m/s is slowed down rapidly, and the crack is arrested within 250 mm in the composite crack arrester. The results of the simulation show a fairly good agreement with the experimental observations, endorsing the use of finite element analysis in the design of crack arrestors for high pressure gas pipelines.

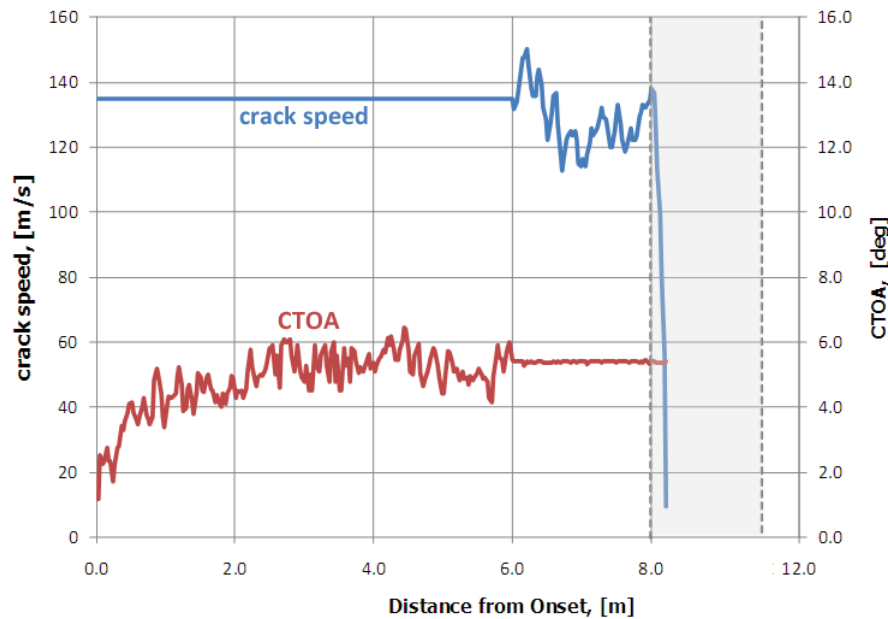


Figure 18: Simulated crack speed diagram for the Demopipe full-scale burst test

6 CONCLUSIONS

Design considerations for crack arrestors used in ultra high grade gas transmission pipelines were reviewed. In [5], unidirectional glass fibre reinforced epoxy was identified as the most promising material for the manufacture of composite crack arrestors. An extensive experimental program was presented to measure the elastic properties of the composite materials. The results from traditional mechanical characterization and non destructive testing were compared. Micromechanical modelling of unidirectional reinforced plastics revealed that the Hashin model is best fit to calculate the stiffness matrix, based on the properties of the fibre reinforcement and the resin.

In this paper, the in-use behaviour of composite crack arrestors was evaluated by means of quasi-static tensile tests and (both monotonic and cyclic) four point bending experiments. The Hashin damage model was applied to predict the onset of composite material degradation. Finite element simulations confirmed that the tensile matrix cracking criterion can accurately predict damage initiation.

In order to assess the ability of composite crack arrestors to stop a running fracture in a high pressure gas pipeline, numerical simulations were performed. The combination of experimental data and finite element analysis allows deriving design guidelines for composite crack arrestors. The design methodology was validated by comparing numerical predictions with the results of a full-scale burst test.

7 ACKNOWLEDGEMENTS

The research results, presented in this paper, were obtained in the scope of the LINESPEC project on *Special Components and Strain Based Requirements for High Strength High Pressure Pipeline Applications*. This project is funded by the Research Fund for Coal and Steel (RFCS).

The authors gratefully acknowledge the support of the project partners BP, SZMF, Corus, ISQ, RWTH and the Soete Lab (UGent).

8 REFERENCES

- [1] Demofonti G. et. Al., Fracture Propagation Resistance Evaluation of X100 TMCP Steel Pipes for High Pressure Gas Transportation Pipelines Using Full Scale Burst Tests, Proceedings of the Fourth International Conference on Pipeline Technology, 9-13 May 2004, Ostend, Belgium
- [2] Mannucci G., Di Biagio M., Demofonti G., Fonzo A., Salvini P. and Edwards A., Crack Arrestor Design by Finite Element Analysis for X100 Gas Transportation Pipelines, Proceedings of the Fourth International Conference on Pipeline Technology, 9-13 May 2004, Ostend, Belgium
- [3] Mannucci G. and Demofonti G., Control of Ductile Fracture Propagation in X80 Gas Linepipe, Proceedings of the Fifth International Conference on Pipeline Technology, 12-14 October 2009, Ostend, Belgium
- [4] Leis B.N., Clark E.B. and Eiber R.J., Crack Arrestor Review – Concepts, Design, Testing and In-Service use, Battelle Institute, Report to BP Exploration and Production (2005)
- [5] Van den Abeele F. and Di Biagio M., Design of Crack Arrestors for Ultra High Grade Gas Transmission Pipelines – Material Selection, Testing and Modelling, Conference on Sustainable Construction and Design, Gent, Belgium, 16-17 February 2011
- [6] Van den Abeele F. and Skocovsky T., Enhanced Failure Criteria for Composite Crack Arrestors, Proceedings of the Fifth International Conference on Pipeline Technology, Ostend, Belgium, 12-14 October 2009
- [7] Van den Abeele F., Amlung L., Di Biagio M. and Zimmermann S., Numerical Design of Composite Crack Arrestors for High Pressure Gas Pipelines, Proceedings of the 8th International Pipeline Conference, IPC2010-31191, Calgary, Canada, September 2010
- [8] ECCS Technical Committee 1, Technical Working Group 1.3, Recommended Testing Procedure for Assessing the Behaviour of Structural Steel Elements under Cyclic Loads, Brussels, Belgium, 1986
- [9] Hashin Z., Failure Criteria for Unidirectional Fibre Composites, Journal of Applied Mechanics, vol. 47, pp. 329-334, 1980
- [10] Hashin Z. and Rotem A., A Fatigue Criterion for Fibre Reinforced Materials, Journal of Composite Materials, vol. 7, pp. 448-464, 1973
- [11] Berardo G., Salvini P., Mannucci G. and Demofonti G., On Longitudinal Propagation of a Ductile Fracture in a Gas Line Pipe: Numerical and Experimental Analysis, Proceedings of the Third International Pipeline Conference IPC2000, Calgary, Canada
- [12] Fonzo A., Salvini P., Di Biagio M. and Mannucci G., Full History Burst Test Through Finite Element Analysis, Proceedings of the Fourth International Pipeline Conference, IPC2002-27120, Calgary, Canada
- [13] Salvini P., Berardo G., Demofonti G. and Mannucci G., Numerical Model of the Backfill Constraint Effect During Fracture Propagation on Buried Large Diameter Gas Pipelines, Proceedings of the Third International Pipeline Conference IPC2000, Calgary, Canada
- [14] Fonzo A., Meleddu A., Di Biagio M., Mannucci G., Demofonti G., Peterson C.W. and Biery N.E., Crack Propagation Modelling and Crack Arrestor Design for X120, Proceedings of the Sixth International Pipeline Conference, IPC2006-10319, Calgary, Canada
- [15] Van den Abeele F., Di Biagio M. and Amlung L., Numerical Design of Composite Crack Arrestors for High Pressure Gas Pipelines, Proceedings of the 8th International Pipeline Conference IPC2010-31191, Calgary, Canada
- [16] Demofonti G., Mannucci G., Di Vito L.F., Aristotile R., Di Biagio M., Malatesta G., Harris D; and Harrison P., Ultra High Strength Pipeline Prototyping for Natural Gas Transmission, Demopipe, EUR 21440 EN, 2003